XIII ICSMFE, 1994, New Delhi, India / XIII CIMSTF, 1994, New Delhi, Inde

BEARING CAPACITY OF CLAY IMPROVED WITH SAND COMPACTION PILES
CAPACITE PORTANTE DE ARGILE AMELIORE AVEC PIEUX DE SABLE

A. Asaoka[1] *M. Matsuo*[1] *T. Kodaka*[2]

[1]Professor, [2]Graduate Student
Department of Civil Engineering
Nagoya University, Nagoya, Japan

SYNOPSIS: The bearing capacity of soft clay improved with sand compaction piles (SCP) is solved here based on the soil-water coupling limit analysis making distinction between undrained and drained condition for sand. When loading by a rigid-rough footing is considered, the drained condition for sand provides big contact pressure concentration on the top of sand piles, which often yields greater bearing capacity than the undrained condition. On the other hand, when embankment-like flexible loading is considered, since no contact pressure concentration should happen, undrained condition for sand gives greater bearing capacity than drained condition due to dilatancy characteristics of sand. Another possible factor that increases bearing capacity of SCP comes from the consolidation of the surrounding clay caused by sand pile driving into the clay, and this problem is also found, in the present study, not to be bypassed at all through examining a field loading test made by the Ministry of Transport of Japan in 1988.

INTRODUCTION

The use of sand compaction piles (SCP) driven into clay thus forming a composite ground, is one of the most effective soil improvement techniques to reinforce and/or strengthen soft clay deposits. The bearing capacity of this type of composite ground has been solved for years by the method of circular-arc slip surface with a given ratio of vertical stress concentration on sand piles. Concerning the strength of soils it has also been assumed in the conventional analysis that the sand follows drained condition, while the clay, undrained. Although the analysis method itself is simple enough for the use in engineering practice, the method can hardly evaluate the following factors that act to bring about the increase of bearing capacity of the composite ground: (1) Stiffness of the load on composite ground, (2) Drainage condition for sand during loading, and (3) Consolidation of surrounding clay due to sand pile driving. The present study provides a simple yet consistent method of solving soil-water coupling limit state of a composite ground to evaluate these three factors quantitatively.

In these years, experimental research works have been accumulated to a considerable extent in order to clarify the failure mechanisms of soft clay improved with SCP through both centrifuge model tests (eg., Kimura et al., 1985; Nakase et al., 1989; Takemura et al., 1990) and a full scale field failure test (Okada et al., 1989). The typical performance observed in these failure tests is also examined and discussed in the present study.

ESSENTIALS OF THE SOIL-WATER COUPLING BEARING CAPACITY ANALYSIS

Stress Strain-rate Relationships at Critical State

Mechanical behaviour of soil is assumed in this paper to follow the original Cam Clay model, from which the stress strain-rate relationship at critical state is obtained as follows:

$$s_{ij} = \left(\sqrt{\frac{2}{3}}\frac{M \cdot (p')_f}{\bar{\dot{e}}}\right) \cdot \dot{\varepsilon}_{ij}^{\,p} \tag{1}$$

in which s_{ij} and p' denote deviatric stress and mean effective stress, respectively while M, the critical state parameter and $\bar{e}$, the equivalent plastic strain rate. It should be noted here that p' at critical state gives *shear strength* of soil and that, since

$$\dot{\varepsilon}_v^{\,p} = 0 \tag{2}$$

the plastic strain rate given in Eq.(1) just follows the plastic flow of the Mises type material.

Limiting Equilibrium Equations

Based on the upper bound theorem in plasticity, the minimization of the rate of plastic energy dissipation at critical state yields the equation of equilibrium of forces:

[*Problem A*] *Some linear relations among velocity components at the displacement boundary are assigned a priori and contact pressure distribution is unknown,* which corresponds to load application through a *rigid rough or smooth* footing. In this problem the equilibrium equation at limit state

$$\int_V B^T s dV + L^T \lambda = C^T \mu \tag{3}$$

should be solved simultaneously with Eqs.(1) and (2) under the following linear constraint condition:

$$C\dot{u} = \dot{u}_0 \tag{4}$$

in which $\dot{u}_0$ is a prescribed velocity, while μ in Eq.(3) represents the contact pressure distribution.

[*Problem B*] *The shape of applied load F has been assigned a priori and the magnitude of applied load μF is unknown,* which corresponds to flexible loading on soft clay. In this problem the equilibrium equation

$$\int_V B^T s dv + L^T \lambda = \mu F \tag{5}$$

should be solved with

$$F^T \dot{u} = 1 \tag{6}$$

where μ is the so-called load factor at limit state. All symbols appeared in Eqs.(3)~(6) follow the usual finite element notation, among which the s and the λ in Eqs.(3) and (5) denote the vector of deviatoric stress and the vector of mean total stress of all elements, respectively.

Coupling Equations

When solving the equation of equilibrium at limit state with constitutive relations Eqs.(1) and (2), an additional field variable $(p')_f$, the mean effective stress at critical state, should be determined simultaneously, which can be performed with the aid of coupling equation that considers volume change behaviour of soil during shear.

When undrained loading is assumed for clay, no volume change condition ($\varepsilon_v{}^e + \varepsilon_v{}^p = 0$) during loading yields the coupling equation:

$$(p')_f = p_0' \exp[\Lambda(-1 + \sqrt{\frac{3}{2}} \frac{\varepsilon_{ij}{}^p \cdot \eta_{ij0}}{M \cdot \dot{\varepsilon}})] \quad (7)$$

in which p_0' and η_{ij0} are the mean effective stress and stress ratio just before undrained loading, respectively and $(p')_f$, the mean effective stress at failure. The Λ in this equation denotes the irreversible ratio defined by $1 - \kappa/\lambda$ where the κ and λ are slopes of swelling and consolidation, respectively.

For compacted sand, the following two drainage conditions are considered during loading.

[*Fully drained and/or swelling case*]

Since no excess pore pressure is assumed to develop, the unknown mean effective stress of sand at failure is simply expressed as

$$(p')_f = (p)_f - \gamma_w \cdot z \quad (8)$$

where $(p)_f$ is the mean total stress at failure and is solved as the element of λ in Eqs.(3) and (5) while $\gamma_w \cdot z$, the hydrostatic pressure. When solving limiting equilibrium equations with the aid of Eqs.(1) and (2), $(p')_f$ is iteratively corrected until Eq.(8) is satisfied (Asaoka and Kodaka, 1992).

[*Undrained case*]

No volume change condition for sand yields

$$(p')_f = p_0' n^{\Lambda} \exp(-\Lambda) \quad (9)$$

in which the degree of compaction of sand is expressed in terms of the *overconsolidation ratio* n defined by

$$n = p_y'/p_0' \quad (10)$$

where p_y' is the mean effective yield stress evaluated in K_0 consolidation condition while p_0', the mean effective stress just before undrained loading. Comparing Eq.(10) with the undrained condition for clay given in Eq.(7), since Λ is positive and $n > 1$, mean effective stress of sand is greater than clay at failure when p_0' is the same. This is, of course, due to the effect of *dilatancy* characteristics of sand observed during shear.

LOADING THROUGH RIGID-ROUGH FOOTING

Load application on the SCP is first considered through a rigid-rough footing, *see* Fig.1, in which plane strain condition is examined for simplicity. Soil parameters of sand and of clay are both tabulated in Table 1, with initial stress distribution. Analyses were equally made for both drained and undrained condition for sand. Ultimate bearing capacity q_f (limit load averaged over the total area of load application)

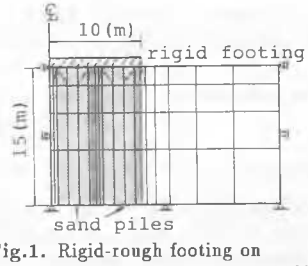

Fig.1. Rigid-rough footing on composite ground, A_S=70%

Table 1. Soil parameters

	λ	κ	M
clay	0.25	0.1304	1.2
sand	0.03	0.003	1.2

$\sigma_v' = 19.6 + \gamma' \cdot z$(kPa)

$\gamma' = 6.37$(kN/m^3)

obtained through a series of analyses is summarized in Fig.2 taking *sand-replacement area ratio* A_S beneath the footing as a parameter.

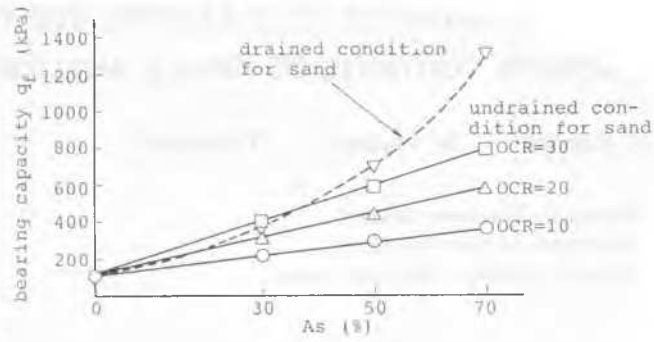

Fig.2. $q_f \sim A_S$

As shown in this figure, when A_S is greater than 40%, a fully drained condition for sand piles gives bearing capacity greater than the undrained condition. This should be due to very high contact pressure concentration on the top of sand piles. The details of the typical example is given in Fig.3 (A_S = 70%), in which the velocity field under the footing is also illustrated. As shown in this figure, the averaged value of the ratio of vertical stress concentration on the top of a sand pile reaches 4.4 or more. Fig.4 shows the vertical stress concentration behaviour with depth, which shows that the stress concentration within sand piles is directly provided through a rigid-rough footing.

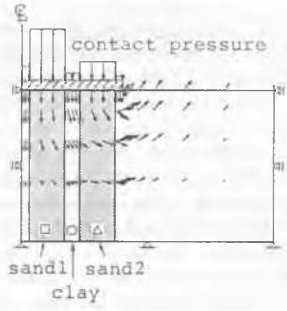

Fig.3. Contact pressure and velocity field, A_S = 70%

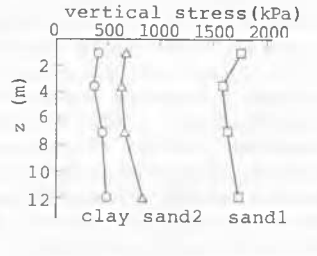

Fig.4. Stress concentration with depth, A_S = 70%

When low sand-replacement area ratio such as A_S < 30% is considered, however, undrained condition for sand provides bearing capacity greater than drained condition. This is much more clearly observed when flexible load application is examined.

EMBANKMENT-LIKE FLEXIBLE LOAD APPLICATION

Here examined is the embankment loading on soft clay in which the area just below the toe of embankment is improved by SCP. No contact pressure concentration is introduced beneath the embankment and the shape of the surface load is assumed similar to the cross-sectional shape of embankment (*Problem B*). In the example problem a relatively low sand-replacement area ratio (A_S = 30%) is considered throughout analyses and the effect of width of improved area on the increase of bearing capacity is examined. The results of analyses are summarized in Fig. 5, in which the same soil parameters and the same initial stress conditions are employed as those for the rigid-rough footing problem. Since there is no contact pressure concentration, undrained assumption for sand always gives greater bearing capacity than the drained assumption.

The shape of shear deformation at failure obtained in the finite element simulation of this study is illustrated in Fig.6, while Fig.7, the failure mechanism observed in centrifuge model test (Takemura, et al., 1991). Model tests and their simulation show that SCP's at the toe of embankment offer a strong registance against lateral deformation.

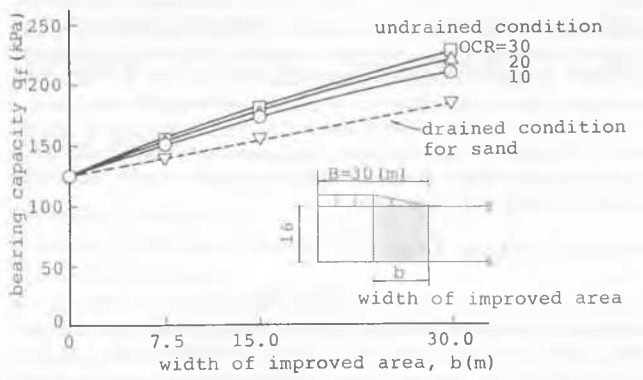

Fig.5. Increase of bearing capacity

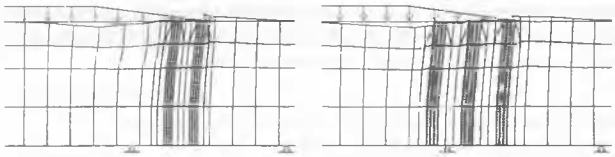

(a) (b)

Fig.6. Shear deformation at failure, (a)b/B=0.25, (b)b/B=0.5.

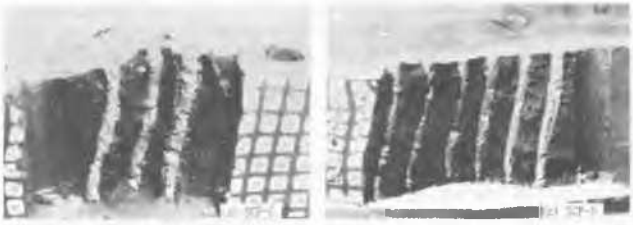

(a) (b)

Fig.7. Failure in model test (Takemura et al., 1991), (a)b/B=0.25, (b)b/B=0.5.

FIELD LOADING TEST TO FAILURE IN MAIZURU, 1988

Profile of the Field Test

A field failure test of composite ground with a relatively low sand-replacement area ratio ($A_S = 25\%$) was conducted in Maizuru, Kyoto by the Ministry of Transport of Japan in 1988, the main purpose of which is to demonstrate that sand compaction piles are still applicable even with such a low sand-replacement ratio (Okada et al., 1989). Shown in Fig.8a is the field test profile with a load application system while in Fig.8b, the failure mode observed in-situ. The loading procedure was made in two stages: (1) After sand pile driving, sand mat fill with a concrete caisson was placed directly on the heaved clay on the composite ground for about ten months. (2) After the ten months, the caisson was filled with sand and a large steel tank was installed on the caisson to apply a vertical force by filling the tank with water. In this second stage the loading was made in nine days and the last 43% of the load was applied rapidly to failure within less than two hours and half in the morning of July 26th, 1988. This loading history is illustrated schematically in Fig.9. A pending technical problem imposed upon engineers in this field test was the evaluation of the undrained shear strength just before the second stage of loading.

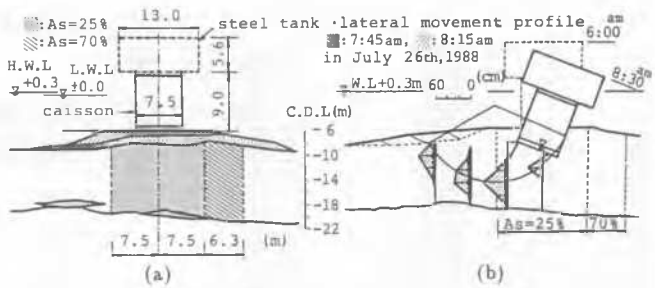

Figs.8. Field test in Maizuru, Kyoto (Okada et al., 1989), (a) First stage of loading,(b) Rapid loading in the second stage to failure.

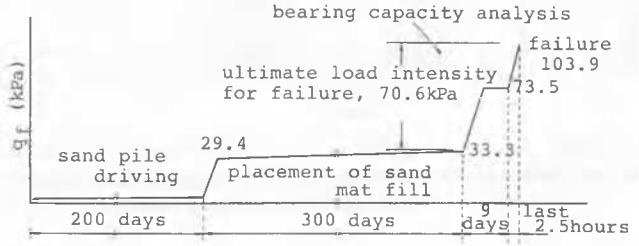

Fig.9. Loading procedure

Consolidation of Surrounding Clay due to Sand Pile Driving

The problem that cannot be bypassed in case of a low sand-replacement area ratio may come from the rapid increase of excess pore pressure in clay due to rapid driving of sand piles, which should initiate the consolidation of surrounding clay and as the results, the increase of both undrained shear strength of clay and confining effective stress for sand piles can both be expected. This is simply called, in this study, the *consolidation effect due to sand pile driving.*

A series of figures given here represents sand pile driving and consequent consolidation of surrouding clay. Pile driving is simulated in the present study by solving a *cylinder expansion problem* in normally consolidated clay, which can be performed by the soil-water coupling limiting equilibrium analysis for clay under undrained condition. Soil parameter and soil profile along depth required for these computation works are given in Table 2, which were determined from in-situ soil conditions at the site of field loading test in Maizuru. Shown in Fig.10a is the plastic flow and *heaving* of surrouding clay due to sand pile expansion from the size of casing to the completed diameter of a sand pile, while excess pore pressure raised just after pile driving is distributed as shown in Fig.10b. Note here that Fig.10b provides the initial condition necessary for the subsequent elasto-plastic consolidation computation. Fig.10c gives the shape of surrounding clay after consolidation together with the setup ratio of undrained shear strength of clay before and after consolidation. Boundary conditions for Figs.10 as well as the period of time for consolidation (*see* Fig.11) were also determined to simulate the field loading test. As can be seen in Fig.11, consolidation of surrouding clay takes considerable time.

Table 2. Soil parameters in Maizuru field test

(Fig.10a)	λ	κ	M	K_0	e_0	γ'(kN/m^3)	k(cm/s)
clay(top)	0.362	0.048	1.20	0.5	2.42	5.29	4.6×10^{-7}
clay(middle)	0.359	0.039	1.27	0.5	1.89	6.27	2.0×10^{-7}
clay(bottom)	0.195	0.025	1.33	0.5	1.37	7.35	6.1×10^{-7}
sand	0.030	0.003	1.20	1.0	-	9.80	-

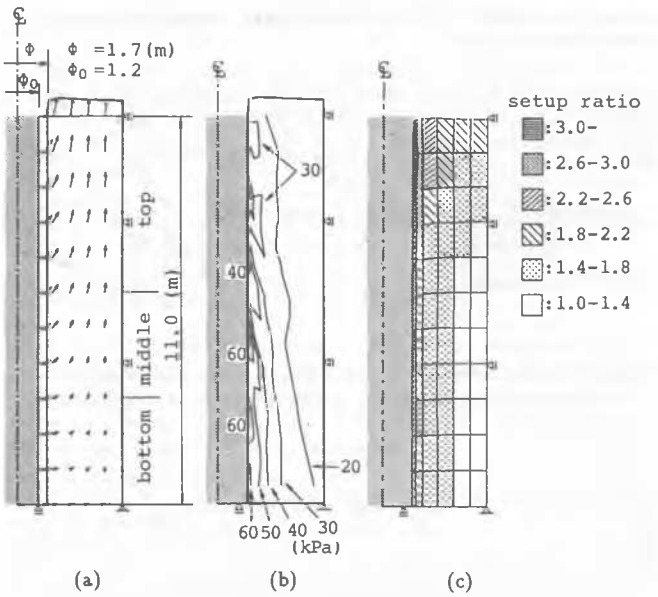

Figs.10. (a) Heaving of clay, (b) Excess pore pressure, (c) Setup ratio of undrained shear strength of clay after consolidation.

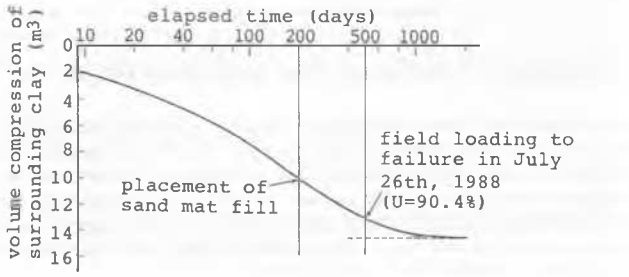

Fig.11. Consolidation with time.

Heaving of the clay that surrounds sand piles also reaches considerable amonnt. Although the height of the heaving is obtained as 50~60cm in computation (*see* Fig.10a), the heave of one meter or more was reported in the case record. When such large shear deformation happens in naturally sedimented clay, since such clay should always be somewhat sensitive, *disturbance effect* on the decrease of shear strength should equally be taken into account. However, the positive effect of consolidation due to sand pile driving is next shown more dominant in the case record.

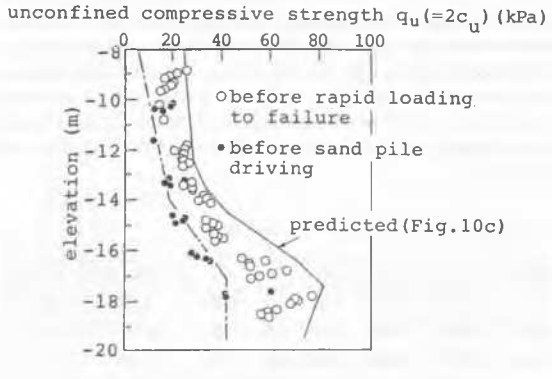

Fig.12. Increase of undrained shear strength of clay.

Fig.12 provides in-situ soil condition measured before sand pile driving and that after the ten month-placement of sand mat fill in the first stage of loading. In this figure, the increased strength profile of clay computed by the consolidation due to sand pile driving (Fig.10c) is also illustrated by a solid line. The computed strength profile gives the strength of clay averaged from pile to pile. As shown in this figure, the computed strength is 20~50% greater than the measured strength at every depth, which suggests the degree of disturbance on the decrease of shear strength of clay. However, it should also be noted that the measured strength still exhibits surprising increase even at a very deep area in the clay, which cannot be explained sufficiently by the conventional conception: consolidation due to the weight of the sand mat fill alone. When SCP with a low sand-replacement area ratio is considered in practice, the increase of shear strength of clay due to sand pile driving is thus identified to be dominant.

Prediction of Limit Load

Summarized in Table 3 are the results of prediction of the ultimate failure load under some different drainage conditions for sand with different degree of compaction. Since a low sand-replacement area ratio (A_S = 25%) is the case, undrained condition for sand predicts higher bearing capacity. The best fit is obtained under undrained condition for sand compacted with $n = 20$. However, drained condition for sand with the use of increased strength of clay also provides sufficient improvement of bearing capacity, which ensure long term stability of composite ground with relatively low sand-replacement area ratio.

Table 3. Prediction of the failure load in the second stage (actual failure load = 70.6 kPa)

undrained analyses	degree of	30	q_f=68.0	(kPa)
for sand	compaction	20	68.0	
	(OCR)	10	63.8	
drained analyses	use of measured strength		52.5	
for sand	(use of predicted strength)		72.2	

CONCLUSION

When rigid-rough footing is considered, drained condition for sand piles provides greater bearing capacity than undrained condition for the sand. To the contrary, embankment-like flexible loading yields greater bearing capacity under the undrained condition. Another factor that increases bearing capacity of soft clay improved with sand compaction piles comes from the consolidation of surrounding clay that should be caused by sand pile driving into the clay, which was found, in a case record study, more dominant than the disturbance effect of soft clay due to the pile driving.

REFERENCES

Asaoka, A. and Kodaka, T.(1992). Seepage failure experiments and their analyses of loose and medium dense sands. *Soils and Foundations* 32(3):

Kimura, T., Nakase, A., Kusakabe, O. and Saitoh, K.(1985). Behavior of soil improved by sand compaction piles. *Proc. of 11th Inter. Conf. on Soil Mech. and Found. Eng.*, San Francisco, Vol.2, pp.1109-1112.

Nakase, A. and Takemura, J.(1989). Stability of clays improved by sand compaction piles, *Tech. Rep.* No.40, Dept. of Civil Engrg., Tokyo Institute of Technology, pp.1-18.

Okada, H., Yagyu, T. and Yukita, Y.(1989). Feild rupture test of soil improved by sand compaction pile method with low sand-replacement ratio. *Tuchi to Kiso* 37(8): 57-62, Proc. JSSMFE (in Japanese)

Takemura, J., Tean, L.B., Suemasa, N., Hirooka, A. and Kimura, T.(1991). Stability of soft clay improved with sand compaction piles under a fill. *Proc. of Geo-Coast '91.*, Yokohama, pp.309-404.